One-Time-Implantable Spinal Cord Stimulation System Prototype

Chia-Hao Hsu, *Student Member, IEEE*, Shao-Bin Tseng, Yi-Jie Hsieh, and Chua-Chin Wang, *Senior Member, IEEE*

***Abstract*—A prototype of a one-time-implantable spinal cord stimulation (SCS) system using wireless power and data-transmission techniques is presented in this paper. The power of the implant is induced by wireless coil coupling, and duplex amplitude-shift keying-load-shift keying wireless communication is used so that digital packets can be transmitted by the same inductive link. The proposed novel ASK demodulator attains high demodulation performance and small area without using any resistors and capacitors. The proposed SCS system utilizes many power saving schemes to reduce power dissipation (e.g., dual supply voltages on-chip, high-voltage impulse generation using small current, etc.). Meanwhile, the excess energy induced by the coils is stored in a rechargeable battery to extend the implant's operation time so that the number of battery replacement surgeries will be reduced significantly. The system-on-chip (SOC) is physically implemented on silicon and integrated in the implant as the system controller. The fabricated SOC area is 1410×1710 μm^2. Compared with existing commercial products, the proposed SCS system attains better flexibility and longer operation time.**

***Index Terms*—Duplex amplitude-shift keying (ASK)–load-shift keying (LSK) communication, spinal cord stimulation (SCS), wireless power transmission.**

I. Introduction

DUE TO THE growth of the aging population, medical disbursement will be very much needed in the foreseeable future. Thus, health care and biomedical markets are expected to be explosively boom in the years to come. Conventionally, electrical stimulation has been used by physicians to assist patients in convalescence. Melzack *et al.* first presented a "gate control" stimulation theory in 1965 [1] describing that the neural mechanism in the dorsal horn of the spinal cord is like a "gate." When the gate is opened by a potentially higher voltage than a threshold voltage, neuron cells are excited in the dorsal horn to transmit pain signals through transmission cells (T cells) to the cerebrum. In contrast, the pathway of pain signals from the neuron fibers is blocked when the gate is closed. Consequently, the pain feeling can be easily reduced by the gate control theory as shown in Fig. 1.

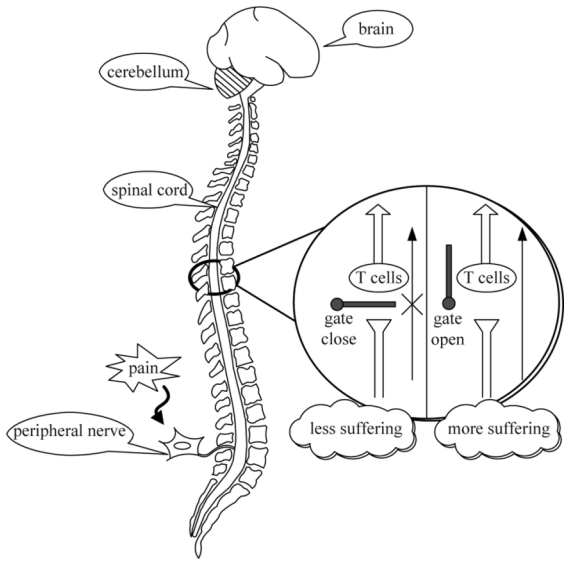

Fig. 1. Gate control theory.

In general, chronically neuropathic pain is caused by neurogenic injure syndromes, such as failed back syndrome, complex regional pain syndrome, arachnoiditis, radiculopathy, and peripheral neuropathy. A spinal cord stimulation (SCS) method was well developed based on the gate control theory to treat the chronically neuropathic pain [2]. Furthermore, [3] presented the analgesic effect in clinical experiments in 1971. Lately, various commercial SCS products are widely implanted in the patients, which are more than 14 000 implementation times worldwide annually [9]. Typically, the stimulating pulses are generated by a pulse generator (PG) in an SCS system providing three kinds of stimulation modes—monopolar, bipolar, and tripolar—to cope with different demands of clinical experiments. The pulse generator usually has four adjustable settings as follows:

1) Pulse amplitude: Setting the threshold voltage of the stimulation signal;
2) Pulsewidth: Setting the stimulated coverage size of the pain area;
3) Stimulation rate: Setting the stimulation impulse time per second;
4) Channel selection: Selecting the output channels of electrodes.

The pulse generator surgically placed under the skin delivers an electrical current or voltage via a lead to the spinal cord. When the pulse generator is turned on, it feels like a mild tingling in the pain area. Notably, experiments show that the reduction of the

Manuscript received December 01, 2010; revised February 22, 2011; accepted May 02, 2011. This work was supported in part by the National Science Council under Grants NSC 99-2221-E-110-081-MY3 and NSC 99-2923-E-110-002-MY2; in part by the Southern Taiwan Science Park Administration (STSPA), Taiwan, under Contract no. EZ-10-09-44-98; and in part by the Ministry of Economic Affairs, Taiwan, under Grants 99-EC-17-A-01-S1-104 and 99-EC-17-A-19-S1-133.

The authors are with the Electrical Engineering Departmernt, National Sun Yat-Sen University, Kaohsiung 80424, Taiwan (e-mail: chhsu@vlsi.ee.nsysu.edu.tw; madabin@vlsi.ee.nsysu.edu.tw; mevis@vlsi.ee.nsysu.edu.tw; ccwang@ee.nsysu.edu.tw).

Color versions of one or more of the figures in this paper are available online at http://ieeexplore.ieee.org.

Digital Object Identifier 10.1109/TBCAS.2011.2157152

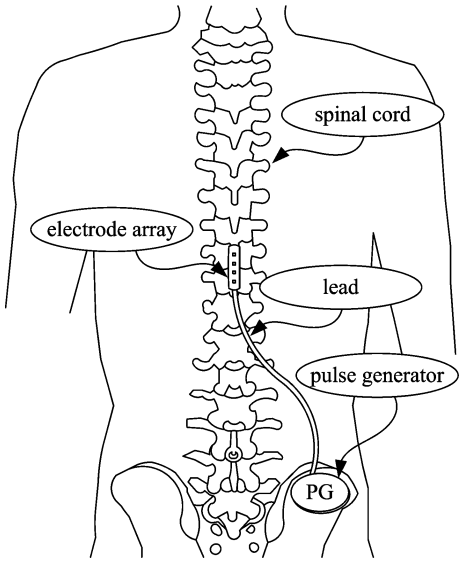

Fig. 2. SCS scenario [20].

pain by SCS is around 70%. Therefore, the SCS technique was justified to effectively reduce the pain. A major advantage is that the possible addiction of patients caused by morphine or opium can be also prevented [10]–[13]. Therefore, the life quality of the patients is then improved by using the SCS technique. Fig. 2 shows the conception of the SCS [20]. The electrode array is inserted in the epidural space of the spinal cord, which is located around the T1 and T2 levels of the spinal cord.

These days, the commercial SCS products are mainly developed by a few major biomedical device companies (i.e., Medtronic, Inc. [15], Boston Scientific Co. [16], and St. Jude Medical, Inc. [17]). The major SCS systems were designed as fully implantable devices. A wireless communication technique is then required to transmit packet and power the implanted device. An even more important point is that the wound infection caused by percutaneous wires can be avoided. A drawback of the pulse generator (PG) is that it needs to be replaced by surgery if the battery is low. Therefore, the reduction of the discomfort caused by the replacement surgery and lifetime extension of the battery become the key research problems of SCS systems. Lately, rechargeable SCS systems using wireless power transmission technique are presented to extend the implant lifetime (e.g., Medtronic RestoreULTRA 37712, Boston Scientific Precision Plus, and St. Jude Medical Eon Mini IPG [15]–[17]). The rechargeable battery of these implantable devices is charged by an outward portable wireless charger. Unfortunately, the portable wireless charger is an independent device, which is inconvenient for patients. For instance, the patients need to carry many devices, which are very space-consuming, and a complicated setting procedure is often needed. Besides, currently commercial SCS products are quite expensive for ordinary patients (e.g., the cost of the commercial SCS products is around U.S.$ 20 000. In the future, commercial SCS products are expected to be of low cost, low power, and small size to benefit more people.

Considering the aforementioned existing issues, this study presents a wireless bidirectional transmission scheme with the power and wireless telemetry capabilities. The PG then generates the stimulation waveforms which imitates neural action potential to achieve pain relief. Fortunately, thanks to the fast evolution of semiconductor and wireless communication technologies, low-cost, low-power, and small-size medical devices can be realized easily. Therefore, the proposed SCS prototype in this paper adopts very-large-scale integrated (VLSI) technology to realize an SCS system-on-chip (SOC) controller in the PG. The power consumption can be reduced by the low-power CMOS circuit design to extend the lifetime of the battery. A lithium-ion (Li-ion) battery is included in the implant to store RF-induced power, where the power is delivered by coil coupling. An *in vitro* experiment has been conducted to illustrate that the proposed design outperforms the existing SCS products.

II. One-Time-Implantable SCS

SCS is a clinical procedure to achieve pain relief as we described in Section I. Conventionally, biomedical electrical stimulation has been categorized in two methods (i.e., current stimulation and voltage stimulation). The current stimulation provides a fixed current impulse to tissues. However, it must overcome high impedance from the tissue, which may weaken driving capability or large power consumption if the distance between two electrodes is far. Besides, larger current may lead tissue burn and may be uncomfortable for the patients when the instantaneous current density is too large which might be caused by unexpected situations. On the other hand, the voltage stimulation can avoid the aforementioned issues of the current stimulation. However, a drawback of the voltage stimulation is that it is hard to give a stable current for the human tissues because the impedance of human tissues is nonlinear and time variant. Notably, the voltage stimulation can avoid the large current causing tissue damage.

Fig. 3 shows the structure of the proposed SCS system. Human skin is located between the outward device (external module) and the inward device (internal module). The bidirectional wireless communication in our system employs an amplitude-shift keying (ASK) and a load-shift keying (LSK) techniques. With the inductive link composed of a pair of coils, the power and the digital packets can be transmitted from the external module to internal module simultaneously. For the other way around, the inductive link can also transmit the internal module's status information to an external module with LSK modulation. In the following subsections, each block in our SCS system is described in detail.

A. External Module

The external module generates carrier waves to transmit the digital packet to the internal module via the inductive link. The external module is composed of an 8051 microcomputer $(\mu\mathrm{C})$, a power transmitter, an LSK demodulator, and an external coil. The 8051 μC generates serial digital packets to the power transmitter according to the configuration settings given by users. The power transmitter modulates the serial digital packets into carrier waves, which are then transmitted by the external coil to internal coil. The LSK demodulator can restore the LSK signal sent by the baseband circuit of the internal module.

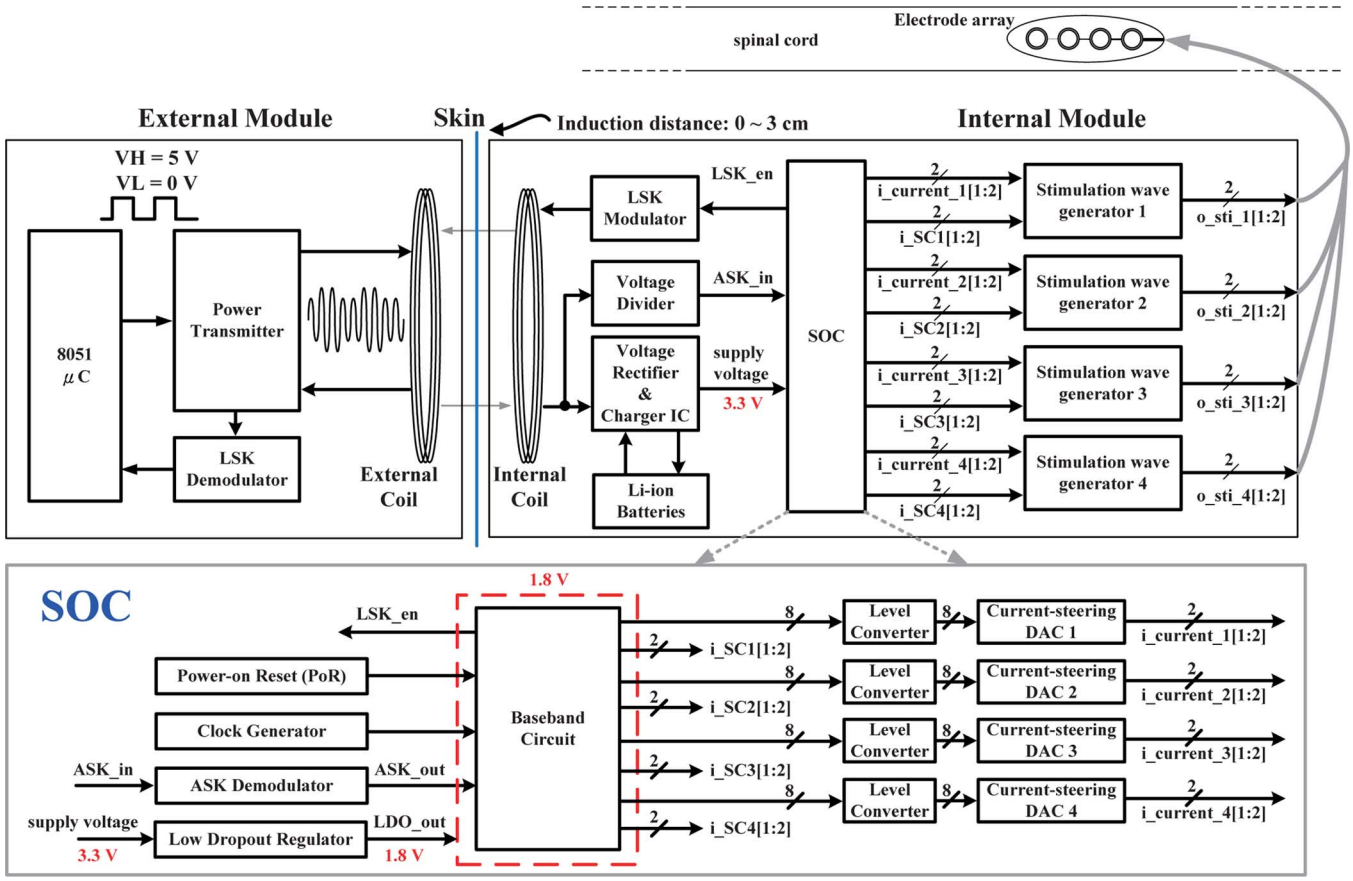

Fig. 3. Block diagram of the proposed SCS system.

1) Power Transmitter: The power transmitter is utilized to carry out power transmission based on an ASK modulation technique [4]. This study proposes a power transmitter with a differential output to attain high efficiency power transmission as shown in Fig. 4, which is composed of a pair of Class-E amplifiers. The digital packet signal, packet_in, from the 8051 μC is used to change the amplitude of the output carrier wave on external coil. Two Darlington pairs—Da1 and Da2—on the two paths are used to provide high current gain, respectively. In path1, the current variation at node A depends on the state of MN1, which causes the emitter current of Q2 to change intensely. When MN2 is switched on, the choke, L1, will inhibit impulses at node B, which is caused by the current variation through L1. To reduce power loss, the switching frequency must operate at the resonant frequency. The resonant frequency ω_p is expressed as follows:

$$\omega_p = \sqrt{\frac{1}{L_E C_1}} = \frac{Q_I R_I}{L_E} \tag{1}$$

where L_E is the inductance of the external coil, and Q_I and R_I are the quality factor and the equivalent resistance of internal coil, respectively.

With a 2-MHz clock signal, clk, to the gate of MN2, node B will generate a carrier wave at the same frequency. On the other hand, the voltage of node C is equal to that of the node B with 180° phase shift due to $\overline{\text{clk}}$, where $\overline{\text{clk}}$ is an out-of-phase

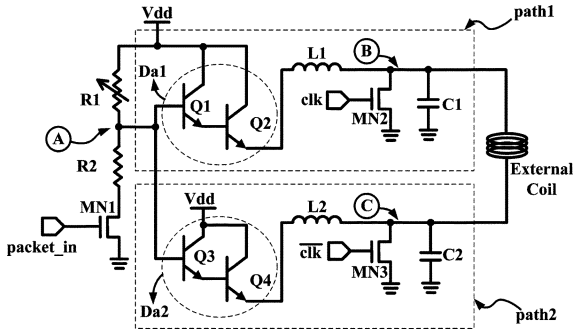

Fig. 4. Schematic of the power transmitter.

signal of clk. By subtracting node C from node B, we can derive a two-time carrier-wave amplitude to enhance the output power on the external coil. Therefore, the carrier wave is generated by mixing the choke-inhibited impulses and packet_in. In short, the frequency of the generated carrier wave is determined by the switching rate of the signals clk and $\overline{\text{clk}}$.

2) LSK Demodulator: The LSK modulation is based on an impedance reflection technique [5], which is used to transmit digital signals without additional coil. The load impedance variation of the internal LSK modulator is reflected to the external coil by the inductive link to cause the resonant frequency shift and amplitude change thereof. The schematic of the proposed

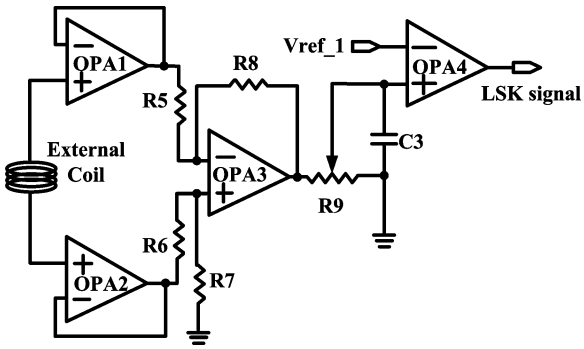

Fig. 5. Schematic of the LSK demodulator.

LSK demodulator is shown in Fig. 5, which can amplify the amplitude variation of the carrier wave. Then, the state of LSK_en in internal module can be reflected at the output, LSK signal.

In Fig. 5, OPA1 and OPA2 are, respectively, unit-gain buffers to duplicate the external coil's signals. Then, the amplitude variation between outputs OPA1 and OPA2 is attained and then amplified by a difference amplifier composed of R5–R8 and OPA3. A low-pass filter composed of R9 and C3 is used to generate a dc potential of the difference amplifier's output signal. Therefore, LSK_en driven by the baseband circuit in the internal module can be recovered at the output of OPA4 (i.e., the LSK signal) by comparison of the dc potential and Vref_1, where Vref_1 is a predefined reference voltage.

B. Internal Module

The internal module is composed of the SOC, the Li-ion battery, stimulation wave generators, and off-chip discretes. According to received configuration setting packets from the external module, the internal module [also known as the pulse generator (PG)] generates corresponding stimulating waveforms to the nerves. The detailed description of each block is described as follows.

1) Charger Integrated Circuit (IC): The proposed SCS system utilizes a commercial charger integrated circuit (IC) (BQ25010) [18] to be a power-management controller. The charger IC will store the excessive power from the RF link into the Li-ion batteries. Besides, the charger IC provides a stable 3.3-V supply voltage to the entire inward SCS system by an integrated low-power high-efficiency dc–dc converter.

2) ASK Demodulator: Fig. 6 shows the proposed novel all-MOS ASK demodulator to demodulate the modulation waves received by the internal coil into digital signals. The received modulation wave is rectified to a dc signal by a half-wave rectifier composed of an MOS diode (Mdiode) and an MOS capacitor (Mcap) in Fig. 6. The headroom of the dc signal is then amplified by the following envelope detector. When dioout is logic high, VP is larger than VN. Venv is then pulled high. Contrarily, Venv is pulled low when $\mathrm{VP} < \mathrm{VN}$. The buffer is used to boost the fan-out capability. Therefore, the received wave is demodulated to be ASK_out, which will be restored and identical to the original digital packets sent from the external module.

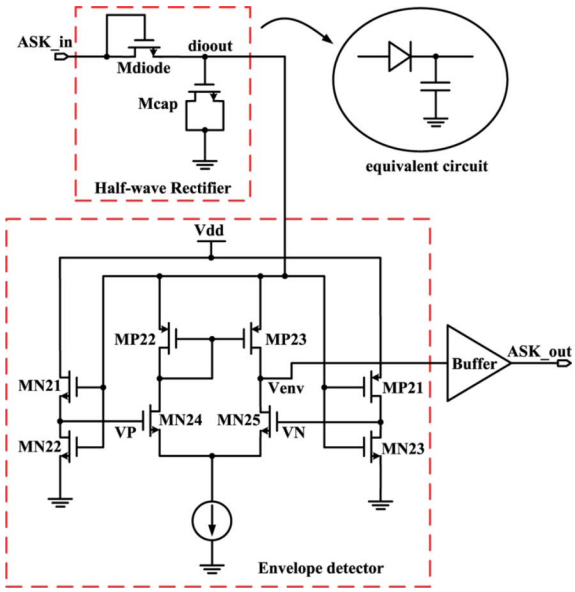

Fig. 6. Schematic of the ASK demodulator.

3) Baseband Circuit: As soon as the received digital packet is demodulated, the baseband circuit generates corresponding stimulating control signals to the off-chip stimulation wave generator 1–4, as shown in Fig. 3. To reduce power dissipation, the baseband circuit employs a 1.8-V supply voltage. The proposed baseband circuit includes a cyclical redundancy check (CRC) error-detecting algorithm [14] to ensure the security of the packet transmission. However, level converters are utilized to translate the stimulating control signals into a 3-V voltage level, which drive four current-steering digital-to-analog converters (DACs) individually. Moreover, the features of the stimulation waves are determined by the baseband circuit, including amplitude, stimulation rate, pulsewidth, etc. [7]. Notably, the low dropout regulator is needed to support the baseband circuit with a 1.8-V supply voltage to reduce power dissipation. Table I tabulates the packet format of the SCS system, where the descriptions of each operation mode are listed as follows.

- Self-test mode: In this mode, it provides a simple self-test capability to verify whether the SOC is working.
- Doctor mode: The parameters of the stimulation waveform (i.e., amplitude, pulsewidth, data rate, and electrode control) are determined by medical personnel in this mode.
- Charge mode: This mode checks the present energy of the Li-ion battery in the SCS system. If the energy is low, it will generate a warning signal.
- Remote mode: The patient can determine the dose time and dose lockout time for the stimulation period.
  Besides, the stimulation procedure is started or stopped in this mode.

4) Current-Steering DAC: Four 8-b current-steering DACs, current-steering DAC 1–4, are used to generate reference currents to stimulation wave generators, respectively. The schematic of the 8-b current-steering DAC 1 is shown in Fig. 7 as an example. Notably, the structures of the 8-b current-steering DAC 2–4 are the same as the 8-b current-steering DAC 1. Stimulation wave generators, respectively, will provide

TABLE I
PACKET FORMAT OF THE SCS SYSTEM

32-bit							
8-bit	2-bit	14-bit					8-bit
Sync character	OP code	Payload					CRC
10101010	self-test mode						Generated by CRC circuit
	00	XXXXXXXXXXXXXX					
	doctor mode						
	01	Amplitude (8-bit)	Rate (6-bit)				
		Pulse width (4-bit)	electrode control (each one is 2-bit)				
			E1	E2	E3	E4	
	charge mode						
	10	101010101010					
	remote mode						
	11	01	Dose time (7-bit)	Dose lockout time (5- bit)			
		1X	XXXXXXXXXXXX				

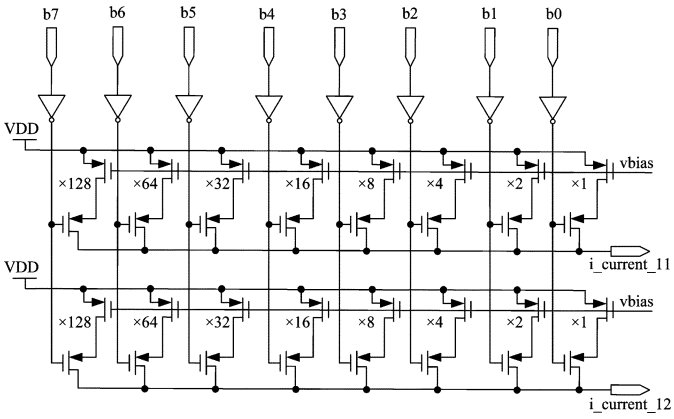

Fig. 7. Schematic of the 8-b current-steering DAC 1.

an appropriate amplitude for stimulating waveforms proportional to their own individual currents.

5) LSK Modulator: We have reported an LSK modulation technique for biomedical wireless communication [6], [8]. After the baseband circuit completes a CRC verification process, the LSK modulator is enabled so that the modulation wave's amplitude of internal coil is changed. The LSK demodulator in the external module can demodulate the modulation wave into a digital waveform with the variation of the amplitude, which then will notify the 8051μC of the status of the internal module.

Fig. 8 shows the concept of the LSK modulation. The voltage on L_E, V_E, can be expressed as (2), where i_1 is the small-signal current of L_E, L_I, and L_E are, respectively, the inductances of internal coil and external coil, and k is the coupling coefficient of L_I and L_E. The impedance Z_2, looking into the LSK modulator from L_1, is shown in (3). When MLSK is on, C_{lsk} is connected in parallel with R_L. The equivalent impedance of the parallel circuit composed of C_{lsk} and R_L is given by (4). On the other hand, R_S is the same as R_L, when the MLSK is off, as shown in (5). Equation (6) is the equation of the coupling coefficient k, where M denotes the mutual inductance. Therefore, the reflected impedance Z_T can be derived by (2) and (3), which is expressed as (7). In summary, the amplitude of the carrier wave on external coil depends on MLSK switching. Thus,

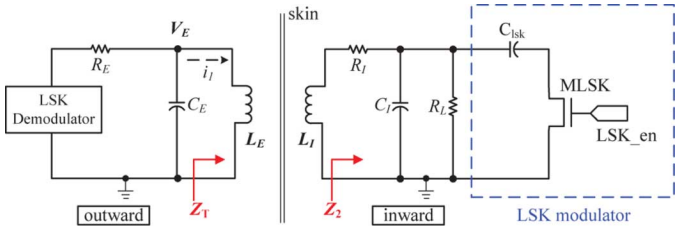

Fig. 8. Concept of the LSK modulation.

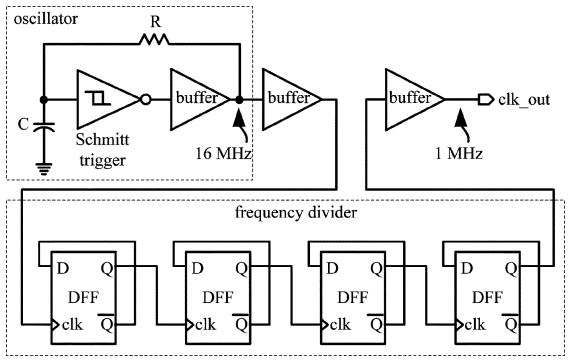

Fig. 9. Schematic of the clock generator.

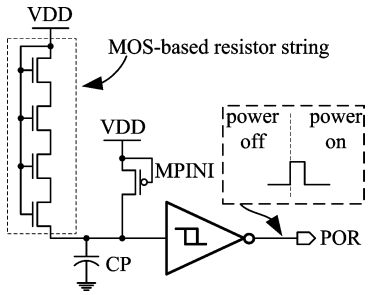

Fig. 10. Schematic of PoR.

the bidirectional wireless communication is realized by the duplex ASK-LSK technique

$$V_E = i_1 \cdot \frac{\omega^2 k^2 \cdot L_E \cdot L_I}{j\omega L_I + Z_2} \tag{2}$$

$$Z_2 = \frac{R_S}{1 + j\omega R_S C_I} + R_I \tag{3}$$

$$R_S = R_L // \frac{1}{j\omega C_{lsk}} \text{ (when MLSK is on)} \tag{4}$$

$$R_S = R_L \text{ (when MLSK is off)} \tag{5}$$

$$k = \frac{M}{\sqrt{L_E \cdot L_I}} \tag{6}$$

$$Z_T = \frac{\omega^2 k^2 \cdot L_E \cdot L_I}{R_I + j\omega L_I + \frac{R_S}{1+j\omega R_S C_I}}. \tag{7}$$

6) Clock Generator and Power-on Reset (PoR): The proposed baseband circuit operates at a 1.0-MHz system clock. A ring oscillator is used to realize the clock generator, which is shown in Fig. 9. The oscillation frequency f_{osc} is determined by the sizes of the resistor and the capacitor, which are given by (8), where V_{SPL} and V_{SPH} are, respectively, the low switching

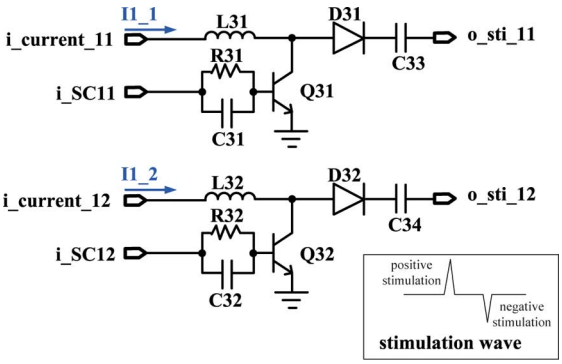

Fig. 11. Schematic of the stimulation wave generators.

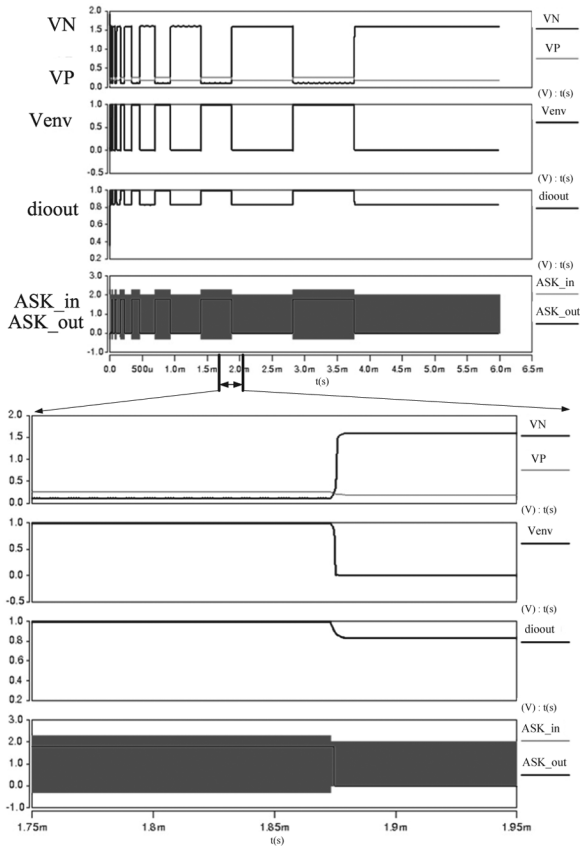

Fig. 12. Simulation of the proposed ASK modulator.

point voltage and high switching point voltage of the Schmitt trigger [19]. Notably, the frequency divider is used to divide the 16-MHz frequency from the oscillator into a 1-MHz output

$$f_{osc} = \left[RC \left(\ln \frac{V_{\mathrm{SPH}}}{V_{\mathrm{SPL}}} + \ln \frac{VDD - V_{\mathrm{SPL}}}{VDD - V_{\mathrm{SPH}}} \right) \right]^{-1}. \quad (8)$$

The proposed PoR circuit is required to avoid any possible unwanted situation (e.g., the race problem at time 0). If the battery is not coupled with the SOC and VDD = 0, CP is discharged through MPINI so that POR is 0. When the VDD is coupled with the battery, MPINI is off and POR is pulled high. Then, CP is charged through the MOS-based resistor string. When CP is charged close to saturation, POR is pulled low. Therefore, the

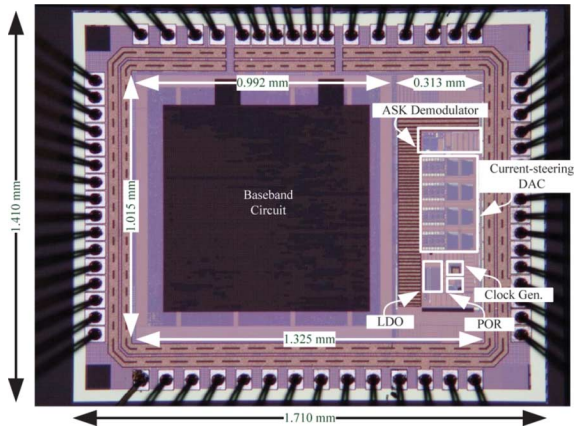

Fig. 13. Die photo of the proposed SCS SOC.

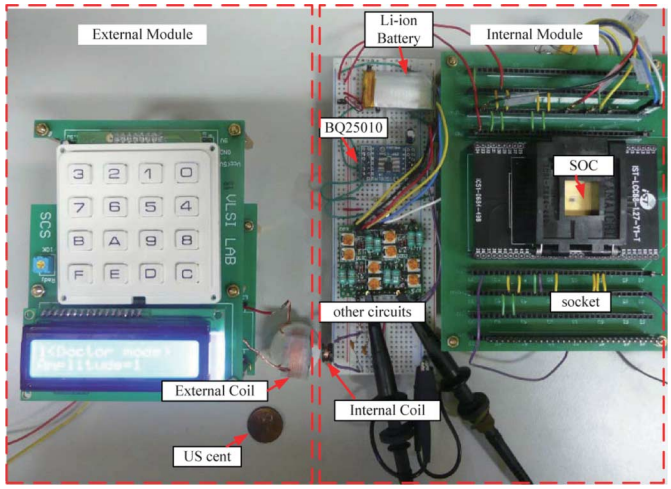

Fig. 14. Photograph of the proposed SCS system.

PoR circuit generates a pulse to reset the SOC into an initial condition.

7) Stimulation Wave Generator: The specification of the required range of the SCS stimulation pulse is as follows: the pulse rate is 2.1 to 130 times per second, the range of pulsewidth is 60 to 450 μs, and the maximum amplitude is around 10 V [7]. The proposed SCS prototype has a 4-channel stimulation array composed of identical stimulation wave generators 1–4. The schematic of the stimulation wave generator 1 is shown in Fig. 11 as an illustrative example, which consists of two independent pulse generators to generate a pair of differential positive and negative stimulation waves. Notably, the spinal cord is stimulated by the positive stimulation wave, and the negative stimulation will neutralize the unwanted spurious charge in the spinal cord.

As shown in Fig. 11, the parallel RC circuit composed of R31 and C31 is used to provide an appropriate current for the base of the bipolar transistor Q31. When the control signal i_SC11, driven by the baseband circuit, is pulled low instantly, a high-voltage impulse is generated at the collector of the bipolar transistor Q31. The high-voltage impulse signal, then, is passed to the output, o_sti_11, through the diode D31 and a capacitor C33. Similarly, o_sti_12 generates another high-voltage impulse driven by i_SC12 from the baseband circuit. Thus, the

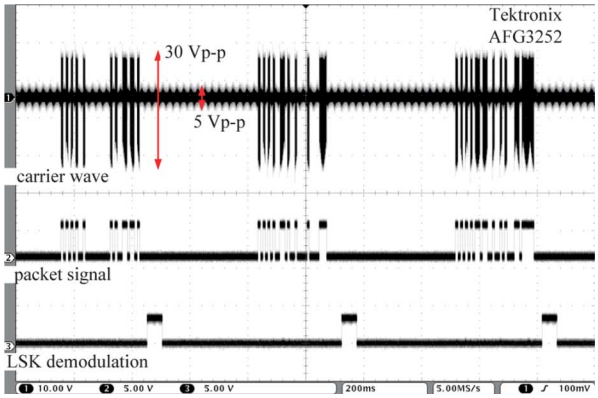

Fig. 15. Measurements of the packet modulation and LSK demodulation.

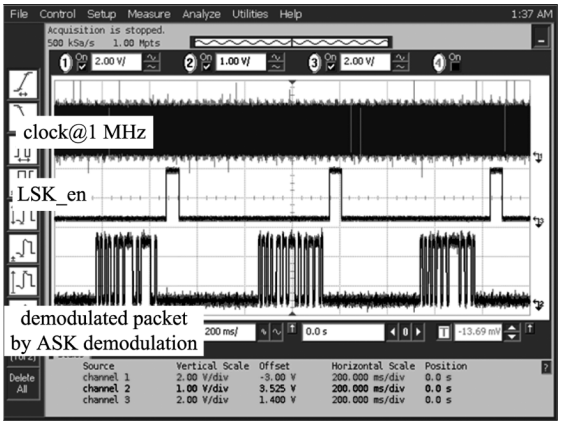

Fig. 16. Measurements of the internal clock, the packet demodulation, and LSK_en.

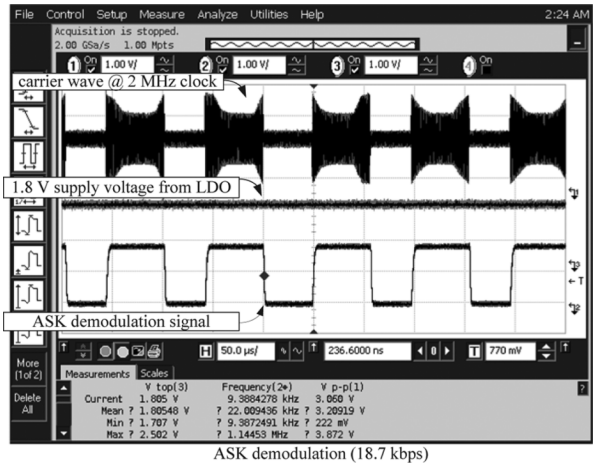

ASK demodulation (18.7 kbps)

Fig. 17. Measurement of the ASK demodulation.

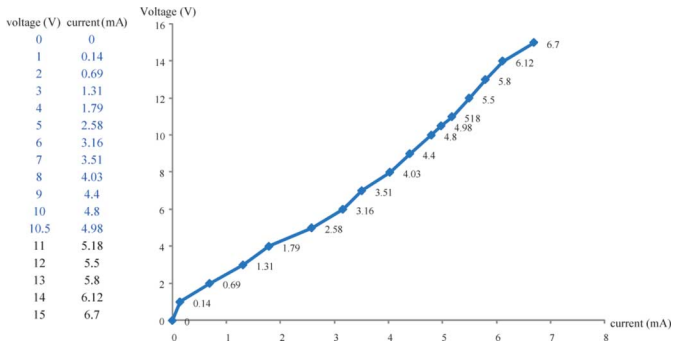

Fig. 18. I–V curve of the stimulation wave generators.

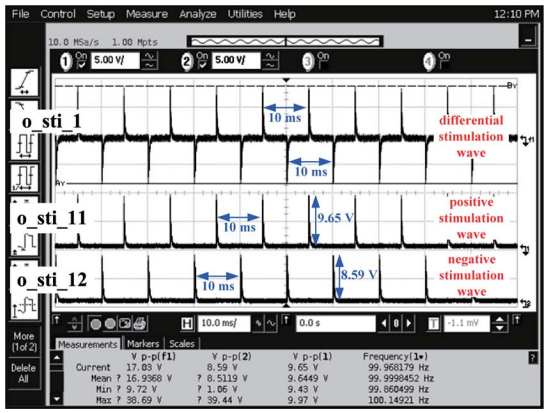

Fig. 19. Measurement of the stimulation wave generator 1.

stimulation wave is generated by the differential signal between o_sti_11 and o_sti_12. Notably, the amplitude of the stimulation wave depends on the input currents i_SC11 and i_SC12 from the current-steering DAC 1. By tuning the i_SC11, i_SC12, i_current_11, and i_current_12, various stimulation waves will be delivered to electrode array via a lead. To meet the flexible application demand, the proposed SCS system provides four independent stimulation wave outputs.

III. Measurement and Implementation

The proposed SOC is carried out on silicon using the Taiwan Semiconductor Manufacturing Company (TSMC) standard 0.18-μm CMOS technology. The simulation result of the proposed ASK demodulator is shown in Fig. 12. When dioout is pulled to 1.0 V, VP is around at 0.3 V, and VN is equal to 0 V (VP $>$ VN). When dioout is 0.8 V, the VP is 0.15 V and VN is pulled to 1.8 V (VP $<$ VN). Thus, the behavior of VP is the opposite of VN. The power consumption of the proposed ASK demodulator is 8.5 μW. Compared with the prior study [21], the proposed ASK demodulator attains lower power consumption ([21] is 306 μW). Fig. 13 shows the die photo of the proposed SOC of the SCS prototype, where the area is 1410×1710 μm^2. The testing instruments adopt an ABM PRT3230 programmable dc power supply and Agilant infiniium oscilloscope. The proposed SCS system prototype is illustrated in Fig. 14.

Fig. 15 shows the packet modulation and LSK demodulation, which is measured by using the Tektronix AFG3252 oscilloscope. The carrier wave is generated by the power transmitter in Fig. 4. When the packet signal from 8051 μC is pulled high, the amplitude of the carrier wave is around 30 Vp-p. Besides, the amplitude of the carrier wave is around 5 Vp-p when the packet signal is pulled low. The demodulated LSK signal on external coil is also shown in Fig. 15. The measurements of packet demodulation and LSK_en are illustrated in Fig. 16. A 1-MHz clock is generated by the clock generator as the system clock of the internal module. The LSK_en is pulled high when the packet from the ASK demodulator passes the CRC verification.

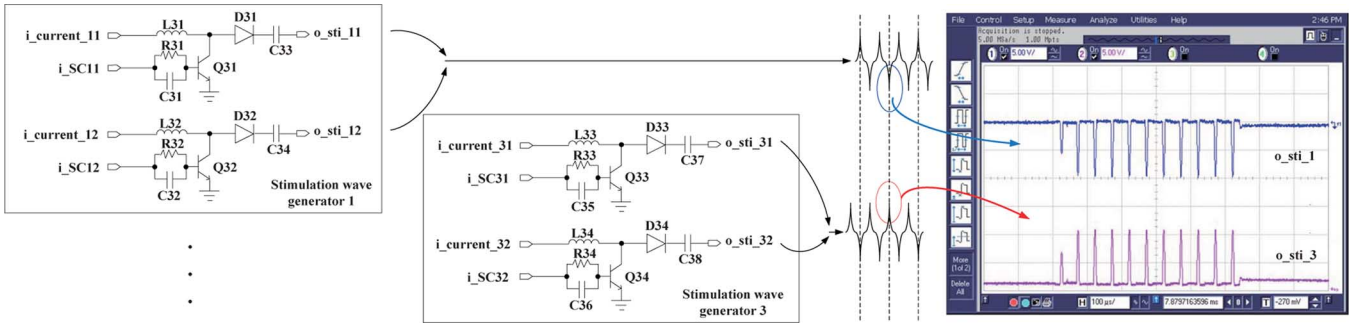

Fig. 20. Expansions of the stimulation impulses.

TABLE II
COMPARISON OF THE COMMERCIAL SCS SYSTEMS

Device	proposed	Medtronic Itrel 3 7425	Medtronic RestoreADVANCED 37713
Max. support electrodes	4	4	16
Stimulation frequency (Hz)	2 $\sim$ 150	2.1 $\sim$ 130	2 $\sim$ 130
Duration of stimulation (minute)	1 $\sim$ 75	15 $\sim$ 75	N/A
Storage temperature (^{o}C)	-18 $\sim$ +52	-18 $\sim$ +52	-18 $\sim$ +52
Amplitude (V)	0.0 $\sim$ 10.5	0.0 $\sim$ 10.5	0.0 $\sim$ 10.5
Pulse width (μs)	60 $\sim$ 450	60 $\sim$ 450	60 $\sim$ 450
Stimulation type	voltage	voltage	voltage
Data rate (throughput)	200 bps	N/A	N/A
RF Band	2.0 MHz	N/A	N/A
Recharge interval (days) (operation in max. power dissipation)	2.13	unrechargeable	1.5
Sleep/Charge/Stimulate mode	Yes	No charge mode	Yes
Rechargeable Battery supported	Yes	No	Yes
Li-ion battery capacity	900 mAh	N/A	N/A
Power dissipation (SOC)	36.96 mW	N/A	N/A
Max. Power dissipation (External Module)	117 mW	N/A	N/A
Max. Power dissipation (Internal Module)	58.08 mW	N/A	N/A

Fig. 17 shows the speed measurement of the ASK demodulator. The proposed ASK demodulator has 18.7 kb/s (bits per second) demodulation capability. Typically, the 200-b/s ASK demodulator is enough to attain the required throughput with 8.5-μW power consumption.

Fig. 18 exhibits the I–V curve of the stimulation wave generator 1–4. The maximum voltage of the output stimulation impulse is 10.5 V in this study, when the input current of the stimulation wave generator 1–4 is 4.98 mA.

Fig. 19 shows the stimulation waves generated by the stimulation wave generator 1. The stimulation wave o_sti_1 is the differential signal between o_sti_11 and o_sti_12, where o_sti_11 and o_sti_12 are 8.59 V and 9.65 V, respectively. Furthermore, the expansions of the stimulation impulses generated by stimulation wave generator 1 and stimulation wave generator 3 are shown in Fig. 20. Each stimulation impulse consists of many small impulses. By controlling the number of the small impulses, the pulsewidth of the stimulation impulse can be adjusted.

Performance comparison with commercial SCS systems is tabulated in Table II. The proposed SCS prototype attains the longest recharge interval using a 900-mAh Li-ion battery. Besides, the setting range of the proposed SCS prototype is more flexible than other existing commercial SCS systems. The volumes of the commercial PGs, Medtronic Itrel 3 7425, and RestoreADVANCED 37713 are, respectively, 22 cm^3 and 39 cm^3. In the future, the target of the proposed internal module will be miniaturized on a printed-circuit board (PCB)-based biocompatible package, which may be smaller than or equal to the size of the commercial PGs.

IV. CONCLUSION

A prototype of a one-time-implantable SCS system is proposed in this paper. To reduce the cost of SCS peripherals, such as the wireless charger, the packet and power of our design can be transmitted by an inductive link by using the duplex ASK-LSK technique via the inductive link. A rechargeable battery is adopted to store the excess power to extend the lifetime of an internal module. Besides, this paper proposes several novel circuits (e.g., ASK demodulator, baseband circuit, power on reset, etc.), which are integrated in the SOC to achieve low power and small area of the implant. The proposed novel ASK demodulator with ultra-low power was compared with the prior design. Besides, compared with the commercial SCS systems, the proposed SCS system has a longer recharge interval. Moreover, the proposed SCS system has a flexible setting range for the generated stimulation waves to meet different stimulation demands.

ACKNOWLEDGMENT

The authors would like to thank the Chip Implementation Center of National Applied Research Laboratories, Taiwan, for their thoughtful chip fabrication service.

REFERENCES

[1] R. Melzack and P. D. Wall, "Pain mechanisms: A new theory," *Science*, vol. 150, no. 699, pp. 971–979, Nov. 1965.

[2] C. N. Shealy, J. T. Mortimer, and J. B. Reswick, "Electrical inhibition of pain by stimulation of the dorsal columns, preliminary clinical report," *Anesthes. Analges., Curr. Res.*, vol. 46, no. 4, pp. 489–491, Jul../Aug. 1967.

[3] K. Shimoji, H. Higashi, T. Kano, S. Asai, and T. Morioka, "Electrical management of intractable pain," *Masui.*, vol. 20, no. 5, pp. 444–447, May 1971.

[4] C.-K. Liang, G.-S. Yang, J.-J. J. Chen, and C.-K. Chen, "A microcontroller-based implantable neuromuscular stimulation system with wireless power and data transmission for animal experiments," *J. Chin. Inst. Eng.*, vol. 26, no. 4, pp. 493–501, Jul. 2003.

[5] G. Gudnason, J. H. Nielsen, E. Bruun, and M. Haugland, "A distributed transducer system for functional electrical stimulation," in *Proc. 8th IEEE Electron. Circuits Syst. Int. Conf.*, Sep. 2001, vol. 1, pp. 397–400.

[6] C.-K. Liang, J.-J. J. Chen, C.-L. Chung, C.-L. Cheng, and C.-C. Wang, "An implantable bi-directional wireless transmission system for transcutaneous biological signal recording," *Physiol. Meas.*, vol. 26, no. 1, pp. 83–97, Feb. 2005.

[7] T. S. Meloy and J. Martin, "Spinal cord stimulation," U.S. Patent 169 924, 2001.

[8] C.-C. Wang, C.-H. Hsu, S.-B. Tseng, and D. Shmilovitz, "A one-time implantable wireless power bidirectional transmission spinal cord stimulation system," in *Proc. Int. Symp. VLSI Design Autom. Test*, Apr. 2010, pp. 288–291.

[9] B. Meyerson and B. Linderoth, "Spinal cord stimulation," in *Loeser JD(ed) Bonica's Management of Pain*, 3rd ed. Philadephia, PA: Lippincott Williams & Wilkins, 2000.

[10] B. A. Meyerson and B. Linderoth, "Mode of action of spinal cord simulation in neuropathic pain," *J. Pain Symptom Manage.*, vol. 31, no. 4S, pp. S6–S12, Apr. 2006.

[11] E. Buchser, A. Durrer, and E. Albrecht, "Spinal cord stimulation for the management of refractory angina pectoris," *J. Pain Symptom Manage.*, vol. 31, no. 4S, pp. S36–S42, Apr. 2006.

[12] D. T. Ubbink and H. Vermeulen, "Spinal cord stimulation for critical leg ischemia: A review of effectiveness and optimal patient selection," *J. Pain Symptom Manage.*, vol. 31, no. 4S, pp. S30–S35, Apr. 2006.

[13] J.-P. Van Buyten, "Neurostimulation for chronic neuropathic back pain in failed back surgery syndrome," *J. Pain Symptom Manage.*, vol. 31, no. 4S, pp. S25–S29, Apr. 2006.

[14] M. E. Kounavis and F. L. Berry, "Novel table lookup-based algorithms for high-performance CRC generation," *IEEE Trans. Comput.*, vol. 57, no. 11, pp. 1550–1560, May 2008.

[15] Networks. Medtronic, Inc., Mar. 2011. [Online]. Available: http://www.medtronic.com

[16] Networks. Boston Scientific Co., Apr. 2011. [Online]. Available: http://www.bostonscientific.com/home.bsci

[17] Networks. St. Jude Medical, Inc., Mar. 2011. [Online]. Available: http://www.sjm.com/

[18] Networks. Texas Instruments, Inc., Dec. 2004. [Online]. Available: http://www.alldatasheet.com/datasheet-pdf/pdf/94247/TI/BQ25010.html

[19] R. J. Baker, "Special purpose CMOS circuits," in *CMOS: Circuit Design, Layout, and Simulation*, 2nd ed. Hoboken, NJ: Wiley, 2005, pp. 521–529.

[20] Networks Mayfield., Feb. 2010. [Online]. Available: http://www.mayfieldclinic.com/PE-STIM.htm

[21] C.-C. Wang, C.-L. Chen, R.-C. Kuo, and D. Shmilovitz, "Self-sampled all-MOS ASK demodulator for lower ISM band applications," *IEEE Trans. Circuits Syst. II, Exp. Briefs*, vol. 57, no. 4, pp. 265–269, Apr. 2010.

Chia-Hao Hsu (S'08) was born in Taiwan in 1981. He received B.S. and M.S. degrees in electronic engineering from Southern Taiwan University, Tainan,, Taiwan, in 2005 and 2007, respectively, and is currently pursuing the Ph.D. degree in electrical engineering at National Sun Yat-Sen University, Kaohsiung, Taiwan.

His recent research interests include very-large-scale integrated design and mixed-signal integrated-circuit design.

Shao-Bin Tseng was born in Taiwan in 1986. He received the B.S. degree in electronic engineering from National Sun Yat-Sen University, Kaohsiung, Taiwan, in 2008, where he is currently pursuing the M.S. degree in electrical engineering.

His recent research interest focuses on very-large-scale integrated design.

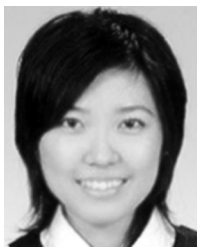

Yi-Jie Hsieh was born in Taiwan in 1984. She received the B.S. degree in optoelectronics communication engineering from National Kaohsiung Normal University, Kaohsiung, Taiwan, in 2006 and is currently pursuing the M.S. degree in electrical engineering from National Sun Yat-Sen University, Kaohsiung, Taiwan.

Chua-Chin Wang (M'90–SM'04) received the Ph.D. degree in electrical engineering from the State University of New York (SUNY), Stony Brook, in 1992.

He then joined the Department of Electrical Engineering, National Sun Yat-Sen University, Taiwan, and became a Full Professor in 1998. He founded the SOC Group, Department of Electrical Engineering, National Sun Yat-Sen University, in 2005, where he is currently Chairman. In 2000, he co-funded Asuka Semiconductor Inc., which is an integrated-circuit (IC) design house located in renowned Hsinchu Scientific Park, Taiwan, and became Executive Secretary in 2005. His research interests include memory and logic circuit design, communication circuit design, neural networks, and interfacing input/output circuits. Particularly, he applies most of his research results to biomedical, memories, consumer electronics, and wireless communication applications, such as implantable application-specific integrated circuit/system-on-chip (ASIC/SOC), digital video broadcasting–terrestrial/handheld (DVB-T/H), and National Television System Committee (NTSC) TV circuits, low-power memory, high-speed digital logic, etc.

Dr. Wang won the Outstanding Youth Engineer Award of the Chinese Engineer Association in 1999 and NSC Research Award from 1994 to 1999. In 2005, he was awarded with the Best Inventor Award at National Sun Yat-Sen University, Taiwan. In 2006, he won the "Distinguished Engineering Professor" Award from the Chinese Institute of Engineers and "Distinguished Engineer" Award from the Chinese Institute of Electrical Engineering in the same year. He also won the Distinguished Electrical Engineering Professor Award from the Chinese Institute of Electrical Engineers in 2007. In 2008, he won the Outstanding Paper Award at the 2008 IEEE International Conference of Consumer Electronics. In 2009, he again won Best Inventor Award. He has served as program committee member in many international conferences. He was Chair of IEEE Circuits and Systems Society (CASS) for 2007 and 2008, Tainan Chapter. He was also the founding Chair of the IEEE Solid-State Circuits Society (SSCS), Tainan Chapter for 2007 and 2008, and the founding Consultant of the IEEE NSYSU Student Branch. He is also a member of the IEEE CASS Multimedia Systems & Applications (MSA), VLSI Systems and Applications (VSA), Nanoelectronics and Giga-scale Systems (NG), and Biomedical Circuits and Systems (BioCAS) technical committees. In 2007, he was elected to be Chair-Elect of the IEEE CASS Nanoelectronics and Giga-scale Systems (NG) Technical Committee to serve a two -year term of 2008–2009. Since 2010, he has been invited to be Associate Editors of IEEE TRANSACTIONS ON CIRCUITS AND SYSTEMS–I: REGULAR PAPERS and IEEE TRANSACTIONS ON CIRCUITS AND SYSTEMS–II: EXPRESS BRIEFS. Currently, he is Associate Editor of *IEICE Transactions on Electronics* and *Journal of Signal Processing*. Dr. Wang was General Chair of the 2007 VLSI/CAD Symposium. He was General Co-Chair of the 2010 IEEE International Symposium on Next-Generation Electronics (2010 ISNE). He is General Chair of the 2011 IEEE International Conference on IC Design and Technology (2011 ICICDT) and General Chair of the 2012 IEEE Asia-Pacific Conference on Circuits & Systems (2012 APCCAS).